



## ISTITUTO NAZIONALE DI RICERCA METROLOGICA Repository Istituzionale

Linearity of a silicon carbide photodiode in the deep-UV spectral region: implications on Doppler broadening thermometry

This is the author's accepted version of the contribution published as:

*Original*

Linearity of a silicon carbide photodiode in the deep-UV spectral region: implications on Doppler broadening thermometry / Dinesan, H.; Gravina, S.; Clivati, C.; Castrillo, A.; Levi, F.; Gianfrani, L.. - In: METROLOGIA. - ISSN 0026-1394. - 57:6(2020), p. 065001. [10.1088/1681-7575/aba052]

*Availability:*

This version is available at: 11696/66121 since: 2021-02-11T16:05:47Z

*Publisher:*

IOP

*Published*

DOI:10.1088/1681-7575/aba052

*Terms of use:*

This article is made available under terms and conditions as specified in the corresponding bibliographic description in the repository

*Publisher copyright*

Institute of Physics Publishing Ltd (IOP)

IOP Publishing Ltd is not responsible for any errors or omissions in this version of the manuscript or any version derived from it. The Version of Record is available online at DOI indicated above

(Article begins on next page)

# Linearity of a silicon carbide photodiode in the deep-UV spectral region: implications on Doppler broadening thermometry

Hemanth Dinesan, Stefania Gravina, Cecilia Clivati, Antonio Castrillo, Filippo Levi and Livio Gianfrani

## Abstract

The linearity of the responsivity of a silicon carbide photodetector in the deep-ultraviolet has been studied using a variant of the so-called intensity-ratio method in view of the implementation of low-uncertainty Doppler-broadening thermometry in mercury vapours. To this purpose, coherent radiation at the wavelength of 254 nm has been produced by means of non-linear mixing of two visible laser beams in a  $\beta$ -barium borate crystal. The linearity has been quantified as a function of the exposure power, variable in the range between 50 and 300 nW. It is shown that possible deviations from linearity are within the uncertainty of  $4 \times 10^{-5}$  (corresponding to one standard deviation). Such a performance makes the detector well suitable for the thermometric application.

## Introduction

The deep-ultraviolet wavelength range is becoming increasingly important in the field of precision spectroscopy for fundamental physics. By using non-linear frequency up-conversion techniques, the remarkable precision of optical frequency combs in the near-infrared can be transferred to the ultraviolet (UV) region [1–3]. So doing, extreme ultraviolet frequency metrology has been recently demonstrated by looking at electronic transitions of molecular hydrogen, which is a benchmark system to test molecular quantum theory [4]. Also, the dissociation energy of ortho- $\text{H}_2$  has been redetermined with an increased accuracy, more than one order of magnitude better than previous measurements [5]. Optical frequency standards are being developed at short wavelengths, with important implications for fundamental metrology, ranging from the redefinition of the second in the International System of Units (SI) to the long term monitoring of a putative variation of fundamental constants [6–8].

The deep-ultraviolet spectral window looks very promising also for the aims of temperature metrology. In fact, Doppler broadening gas thermometry (DBT) can be implemented by probing the  $6s^2\ ^1\text{S}_0 \rightarrow 6s6p\ ^3\text{P}_1$  intercombination transition in mercury vapours, at the wavelength of 253.7 nm. This line, normally used for laser cooling of Hg atoms [7], is an ideal candidate to perform DBT for a variety of favourable features. The mercury vapour pressure at temperatures nearby the triple point of water is of the order of  $10^{-2}$  Pa. Therefore, any collisional perturbation to the shape of the intercombination line can be completely neglected, circumstance that simplifies enormously the spectral analysis for temperature retrieval. At the same time, due to the high value of the Einstein coefficient, large absorption of UV radiation is expected in coincidence with the line centre frequency. Moreover, the lifetime of the excited  $^3\text{P}_1$  level and, consequently, the natural broadening of the line are well known [9]. Most importantly, the ratio between the Doppler width and the homogenous width of the intercombination line is of the order of 750, namely, much larger than that of other atomic lines, already experienced in DBT experiments [10, 11]. It is useful to remind that this ratio is of the utmost importance for low uncertainty determinations of thermodynamic temperatures by means of DBT [12]. As it is well known, the highly accurate observation of the shape of an atomic or molecular spectral line is an indispensable prerequisite for the successful operation of Doppler broadening thermometry. This makes optical detection a very critical point for any DBT experiment, with a particular focus on the linearity of the responsivity and noise level at small powers. The responsivity of an optical detector is defined as the ratio of its output electric signal to input radiometric quantity. A detector is called linear if its responsivity does not vary with the amount of input radiation.

Silicon-carbide (SiC) photodiodes represent the device of choice for the deep-ultraviolet wavelength region for some unique properties. The wide bandgap of 3.26 eV of the 4H polytype at room temperature, corresponding to a wavelength of 380 nm [13], makes it possible the construction of pin-photodiodes that are visible blind, with a blindness larger than  $10^{10}$  for wavelengths greater than 405 nm. Commercially available since more than one decade, these photodiodes are ideally suited for high-sensitivity applications because of the relatively high responsivity (of about  $0.1\ \text{A W}^{-1}$  at 280 nm), large shunt resistance and the low dark current, which lies in the sub-pA range at room temperature [14]. Instead, photomultipliers or silicon based photodiodes usually have relatively low quantum efficiency for deep-ultraviolet radiation and exhibit very broad spectral responsivity, which makes them sensitive also to higher wavelengths. As far as the response linearity is concerned, Si detectors exhibit an excellent performance, with a linearity over the photocurrent range from  $10^{-11}$  to  $10^{-3}$  A within the expanded uncertainty (corresponding to 2 standard deviations) of 0.054% [15]. To the best of authors' knowledge, no quantitative information is available on the linearity of the responsivity of SiC photodiodes.

Two common methods can be implemented to check the linearity, namely, the flux-ratio method and the beam flux addition method (also known as the superposition method) [16]. The former is based on the attenuation of the optical power by inserting filters on the optical path, and measuring the possible change in filter-in to filter-out signal ratios [17]. The latter technique consists in splitting a source beam into two parts, variably attenuating one of the two and recombining them at the photodetector, which sees the sum of the two fluxes,  $\Phi_1 + \Phi_2$ . If  $y(\Phi)$  is the response function of the detector, the flux addition method delivers the ratio  $[y(\Phi_1) + y(\Phi_2)]/y(\Phi_1 + \Phi_2)$  [18]. A possible deviation of this ratio from unity quantifies the non-linearity of the responsivity of the test detector.

In this work, we report the results of a linearity test performed on a SiC detector, using coherent radiation at 254 nm, produced by Sum Frequency Generation (SFG) of two diode lasers in the visible. As clearly stated in [18], there is a danger in the superposition method when deriving the two fluxes from a single source: the coherence between the two fluxes may cause errors in measuring the non-linearity due to interference effects. For this reason, we preferred to avoid resorting to the flux addition method, thus implementing a variant of the flux-ratio method.

We determine the so-called linearity factor at the specific wavelength of interest, in the UV power range that is useful for the aims of Doppler broadening thermometry. It is worth noting that the purpose of our work is not the determination of the non-linearity correction factor that would be useful for absolute radiometry. In fact, we intend to manage the possible non-linearity of the SiC photodiode as a performance limitation to be considered in the DBT experiment on Hg vapors.

### Experimental apparatus

The experimental set-up is shown in figure 1. We implemented a scheme similar to that discussed in [19], using a pair of extended cavity diode lasers (ECDL), emitting in the blue and red regions.

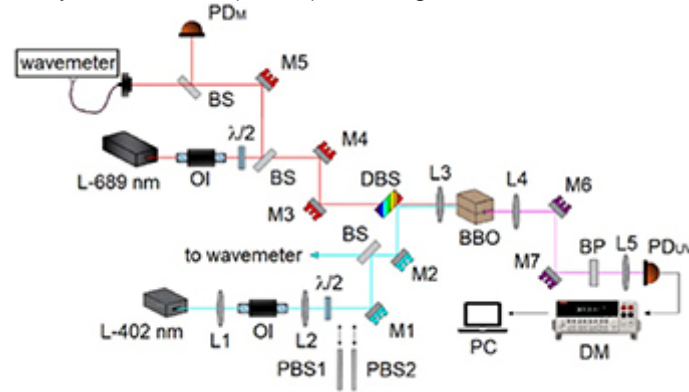


**Figure 1.** Sketch of the experimental apparatus. L stands for lens; OI, optical isolator;  $\lambda/2$ , half-wave plate; BS, beam splitter; M, mirrors; DBS, dichroic beam splitter; PBS, pellicle beam splitter; PDM, monitor photodiode; PDUV, SiC photodiode; BP, bandpass filter; BBO,  $\beta$ -barium borate crystal; DM, digital multimeter; PC, personal computer.

The blue laser (from MOGLabs, LDL 402) operates in the Littrow configuration at the wavelength of 402 nm, with an output power up to 60 mW, a mode-hop free tuning range of 20 GHz and a free-running linewidth of about 200 kHz. Mounted on a monoblock chassis and characterized by the absence of coil springs and flexures, this ECDL is extremely compact, robust, stable, and vibrationally inert. The red laser (Atom Sensors AS689-L) is a master oscillator power amplifier (MOPA) in which the seed laser is an ECDL at 689 nm and a tapered amplifier boosts the optical power up to 180 mW, with a free-running emission linewidth of about 300 kHz. The polarization of the two beams was accurately set in the vertical position by means of a pair of half-wave plates. Mode-matching between the two lasers was quite critical, due to the bad quality of the transverse mode at the output of the tapered amplifier. The two beams are spatially overlapped at a dichroic mirror and focused by a  $f = 50$  mm focal-length lens into a  $\beta$ -barium borate (BBO) crystal (CASTECH), which produces coherent radiation at the sum of the two input frequencies when the type I phase-matching condition is achieved. The 12-mm long crystal is cut at  $\theta = 49.1^\circ$  and its input and output facets present an anti-reflection (AR) coating at 254 nm, along with a broadband coating in the visible. The crystal is mounted on a rotation stage for achieving the phase-matching condition through angle-tuning. The crystal mount is constantly kept at the temperature of 50 °C by means of a Peltier element, in order to avoid water vapour condensation on the crystal facets. Active temperature stabilization is performed at the level of 0.01 °C by using a proportional-integrative-derivative controller. After collimation, the SFG output is filtered by means of a bandpass filter

(Semrock FF01-254/8-25) to block the residual blue component, and gently focused on a SiC photodiode from Sglux, model TOCON\_C6 (with UVC filter and active area of 0.50 mm<sup>2</sup>), operating at room temperature. Such a detector is equipped with a transimpedance preamplifier based upon the Texas Instruments LMC6001 device. Voltage signal acquisitions are performed by means of a 6½-digit multimeter (Keithley 2700), which is remotely controlled by a LABVIEW code through a USB/GPIB board.

Assuming a lossless crystal and a focused Gaussian beam with a circular transverse section, the generated UV power is given by [20]:

$$P = \frac{4\omega_1\omega_2\omega_3 d_{eff}^2 P_1 P_2 l h_3}{\pi \epsilon_0 c^4 n_3^2}, \quad (1)$$

where  $\omega_1$  and  $\omega_2$  are the angular frequencies of the incident laser beams,  $\omega_3 = \omega_1 + \omega_2$  is the UV angular frequency,  $d_{eff}$  is the effective second order non-linear susceptibility coefficient,  $P_1$  and  $P_2$  are the incident powers,  $l$  is the crystal length,  $h_3$  is a dimensionless focusing parameter,  $n_3$  is the crystal refractive index at the UV wavelength and  $c$  is the vacuum speed of light. The effective value of the non-linear susceptibility tensor is calculated to be 1.57 pm V<sup>-1</sup> by means of the expression for a negative uniaxial crystal of class 3 *m* under type I phase matching condition. We have assigned  $h_3 = 0.01$  that is a reasonable value in the case of strong focusing. The refractive index of the crystal at 254 nm amounts to 1.62 according to the Sellmeier equations [20]. For the operation power levels of  $P_1 = 15$  mW for the blue laser and  $P_2 = 120$  mW for the red one, the expected UV power results to be 340 nW. Accounting for the 70% transmission of the bandpass filter before the detector, we expect to measure a UV power of about 240 nW. Instead, we recorded a UV power level of 120 nW. The disagreement is mostly due to the imperfect mode-matching of the two lasers. However, by increasing the input powers, we could measure up to 400 nW (as measured before the bandpass filter) of coherent radiation at 254 nm. Such a power is sufficiently high for the aims of precision, Doppler-limited, absorption spectroscopy in mercury vapours, as demonstrated in figure 2, which shows the shape of the 6s<sup>2</sup> <sup>1</sup>S<sub>0</sub> → 6s6p <sup>3</sup>P<sub>1</sub> intercombination transition of the <sup>200</sup>Hg and <sup>202</sup>Hg bosonic isotopes at 253.7 nm. This recording was performed after inserting a 2-cm long mercury vapour cell, at room temperature, in the beam path between the crystal and the SiC detector. Probing these lines with a larger UV power would lead to measurable perturbations to the lineshape caused by spectral power broadening and optical saturation effects [11]. In this respect, the key parameter is the saturation intensity that amounts to about 5 mW cm<sup>-2</sup> for the mercury line of interest. This value translates into a saturation power of about 6 mW for the collimated UV beam.

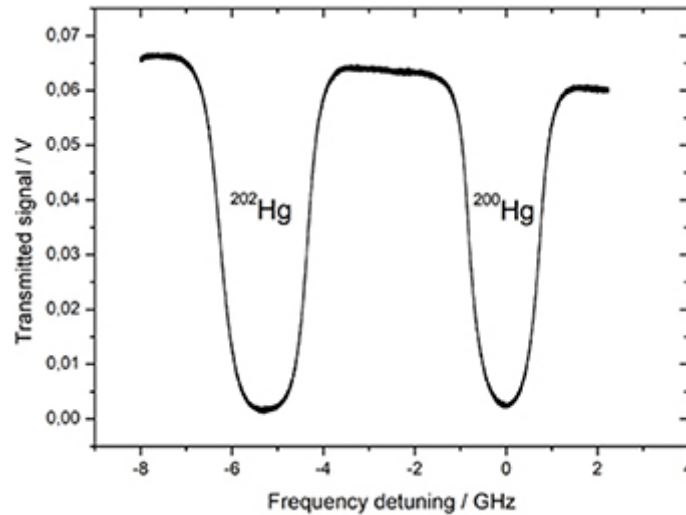


**Figure 2.** Spectroscopy of the 6s<sup>2</sup> <sup>1</sup>S<sub>0</sub> → 6s6p <sup>3</sup>P<sub>1</sub> transition in mercury vapours at room temperature. The line centre fractional absorption is larger than 90% for both isotopes.

It is worth noting that all the optical components (lenses, optical isolators and half-wave plates) have high-quality narrow-band AR-coatings at the specific wavelength of operation, thus avoiding the occurrence of spurious etalon effects.

## Results

A variant of the flux-ratio method was implemented, drawing inspiration from [21]. The blue laser beam was attenuated by using a pair of pellicle beam splitters (PBS) with transmissions,  $T_1$  and  $T_2$ , of 70% and 90%,

respectively, for s-polarized light, thus producing a sequence of four different UV powers incident upon the SiC photodetector. The use of pellicle beam splitters (Thorlabs, BP108) is crucial to preserve the optimal alignment of the blue laser. They are mounted on precision translation stages so as it is possible to remove and reinsert them in the beam path always in the same position, also ensuring a constant angle of incidence (of about 45°). Therefore, in our set-up there is no superposition of two parts derived from the same flux. Since the transmission coefficient of the two combined PBSs is equal to the product of the transmission coefficients of each PBS, the following equation holds:

$$\frac{\Phi_3 \Phi_0}{\Phi_1 \Phi_2} = 1, \quad (2)$$

where  $\Phi_0$  is the blue flux with no attenuation,  $\Phi_1$  the flux with a first PBS alone on the beam path of the blue laser,  $\Phi_2$  refers to the second PBS alone and, finally,  $\Phi_3$  is the flux with both PBSs in action. The same equation is valid also for the UV fluxes, provided that the power of the red beam is kept constant. In case of a perfect linear behaviour of the SiC photodiode, the detector signals,  $S_i$ , with  $i = 0, 1, 2, 3$ , obey to a similar equation. Therefore, a deviation from unity of the ratio  $S_3 S_0 / (S_1 S_2)$  indicates a non-linearity in the detector's responsivity. This approach requires a stable power for the UV radiation and, consequently, a stable emission from both visible lasers over the time span necessary for the acquisition of the signals' sequence, which amounts to about 20 min. The blue laser satisfies this requirement. In fact, as a result of a stability test, we measured a relative power variation of about  $5 \times 10^{-6}$  over one hour. For the red laser we observed a worse performance. In order to compensate for possible systematics caused by these power instabilities and drifts, a monitor Si detector probed continuously the red-laser output power.

Hence, the digital multimeter was configured so as to measure the ratio between two voltages, namely,  $S_i/M_i$ ,  $M_i$  being the monitor signal. Correction for the dark signal of the SiC detector was performed in each configuration of the sequence.

The quantity of interest is the so-called linearity factor,  $\epsilon$ , which can be expressed as a sort of super-ratio, according to the following equation:

$$\epsilon = \frac{\frac{S_3}{M_3} \frac{S_0}{M_0}}{\frac{S_2}{M_2} \frac{S_1}{M_1}}. \quad (3)$$

This quantity was determined as a function of the UV power impinging the SiC detector, which was varied between 50 and 300 nW by changing the injection current of the tapered amplifier as well as the power of the blue laser. For each UV power value, twenty repeated acquisitions were performed, each time removing the PBSs and repeating the sequence. A set of measurements is shown in figure 3(a) to give an example of the reproducibility of our procedure. Each point results from equation (3), using mean values of  $S_i/M_i$  over 100 repeated determinations, while the uncertainty bars are given by the propagation of the standard deviations of the  $S_i/M_i$  ratios. The mean value of these data amounts to 1.00003 (18). Similar results were obtained in the whole range of UV powers investigated in the present work. In figure 3(b), the linearity test results are shown. On the horizontal axis of this plot, we report the mean value of the photocurrents, as measured in each sequence. A weighted linear fit to these values in the exposure range gives a slope and an intercept consistent with zero and one, respectively, within one standard deviation, circumstance that demonstrates the linearity of the responsivity. In order to quantify the linearity, we used the weighted mean of the data of figure 3(b), which amounts to 0.99997 (4). The uncertainty on the mean, which gives the upper limit to a possible deviation from linearity, is more than a factor of 10 smaller than that of [15]. However, a more significant comparison with silicon photodiodes would require a much wider exposure range for the SiC detector, which is far from the scopes of the present article.

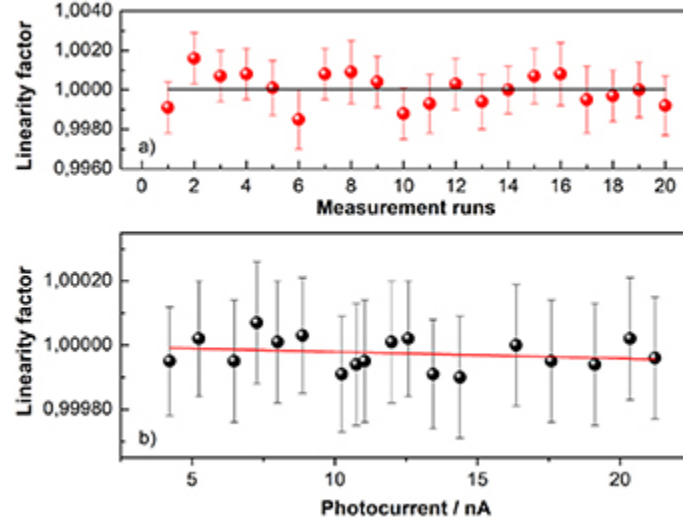


**Figure 3.** (a) Repeated determinations of  $\epsilon$  at an incident power of 120 nW. The multimeter gatetime was set to 1 s. (b) Linearity factors of the SiC detector as a function of the photocurrent, for an exposure range from 50 nW to 300 nW; the best-fit line (in red), which was found by fixing the intercept at one, shows a slope consistent with zero within the uncertainty of  $8.7 \times 10^{-7} \text{ nA}^{-1}$ .

As for possible sources of type-B uncertainties, influencing the determination of  $\epsilon$ , we should mention interference effects. More particularly, our detector is mounted in a hermetically sealed metal package with a melted window. The usage of a coherent source may cause an etalon effect between the window and the SiC active region, with a free-spectral-range between 100 and 200 GHz. Nevertheless, frequency drifts of the laser system over the typical time span of our acquisitions resulted to be much smaller than this value (namely, at the level of a few MHz), so that any spurious modulation of the signal was well within the noise level. Similarly, we looked for other spurious etalon effects by repeatedly scanning the laser frequency. Also in this case, we did not observe any periodic amplitude modulation that could be ascribed to an interference effect, even doing signal averaging over tens of acquisitions. Another source of type-B uncertainty might be the transimpedance amplifier. Since the mean linearity factor is consistent with one, we are confident that possible deviations due to a non-linearity of the amplifier should be well within the type-A uncertainty. Finally, the digital multimeter shows an analog-to-digital linearity with an uncertainty of  $10^{-6}$  of reading. For this reason, its contribution to the budget of uncertainties can be neglected.

### Implications for Doppler broadening thermometry

In order to quantify the influence of a possible detector non-linearity on DBT, a procedure similar to that described in [22] was adopted. Using the Beer–Lambert law, absorption spectra across the intercombination transition of the  $^{200}\text{Hg}$  isotope were simulated for different values of the cell's length,  $L$ , according to the following formula:

$$P_t(\nu) = P_{in} e^{-\alpha(\nu)L}, \quad (4)$$

$P_{in}$  and  $P_t$  being the UV power at the entrance and at the exit of the mercury cell, respectively. A Gaussian function with a Doppler width of 494 MHz (half width at half maximum, for mercury vapours at  $T = 273.15 \text{ K}$ ) was used to describe the dependence of the absorption coefficient,  $\alpha$ , on the laser frequency,  $\nu$ . The simulated spectra were characterized by a line centre fractional absorption,  $\Delta P/P_{in}$ , variable from 26% (for  $L = 0.3 \text{ cm}$ ) to 87% (for  $L = 2 \text{ cm}$ ). Then, a non-linear detector signal,  $S$ , was calculated under the assumption of a linearity factor decreasing linearly with the incident flux, namely,  $\epsilon = 1 - k\Phi$  [23]. The best-fit line of figure 3(b) was found by setting the intercept at one. Its slope was consistent with zero within the uncertainty of  $8.7 \times 10^{-7} \text{ nA}^{-1}$ , which translates into an uncertainty on  $k$  of  $7.8 \times 10^{-8} \text{ nW}^{-1}$  (the estimated value for the mean responsivity being  $0.09 \text{ A W}^{-1}$ ). Therefore, with a linear dependence of the responsivity on the optical flux, the signal is given by

$$S = \Phi R_0 (1 - \beta \Phi), \quad (5)$$

where  $R_0$  is a constant factor, while the quantity  $\beta$  can be easily calculated from equations (2) and (3). In other words, it is possible to find the  $\beta$ -factor so that the following condition is satisfied:

$$\frac{(1 - \beta\Phi_3)(1 - \beta\Phi_0)}{(1 - \beta\Phi_1)(1 - \beta\Phi_2)} = 1 - k\Phi, \quad (6)$$

under the assumption of a constant monitor signal ( $M_0 = M_1 = M_2 = M_3$ ). It is worth noting that the quantity  $1 - \beta\Phi$  has the meaning of a non-linearity correction factor. After some approximations, the following expression can be found:

$$\beta = \frac{k}{1 + T_1T_2 - T_1 - T_2} \quad (7)$$

Setting  $k$  equal to its uncertainty, the equation above yields  $\beta = 2.6 \times 10^{-6} \text{ nW}^{-1}$ . This latter represents an upper limit to the coefficient that adds a non-linearity to the detector signal.

Since the UV flux shining on the detector comes to coincide with  $P_i$ , distorted spectra can be simulated by using the following equation:

$$S(\nu) = P_{in}e^{-\alpha(\nu)L}R_0 \left[ 1 - \beta P_{in}e^{-\alpha(\nu)L} \right]. \quad (8)$$

Then, a non-linear least-squares fit of the distorted profiles was performed using a Gaussian shape with the Doppler width treated as a free parameter, so that it was possible to calculate the relative deviation,  $\delta_D$ , of the retrieved value with respect to the simulated one. These deviations should be considered as upper limits. Table 1 resumes the overall results. It is clear that the systematic shift on the retrieved Doppler width can be reduced down to the target part-per-million level with a proper combination of absorption pathlength and incident flux.

**Table 1.** The impact of a possible detector non-linearity on DBT.

$P_{in} / \text{nW}$	Absorption pathlength/cm	$\Delta P / P_{in} / \%$	$\delta_D / \text{parts per million}$
10	2	87	2.8
10	1	63	2.1
10	0.5	40	1.3
50	2	87	13.8
50	0.5	40	6.7
50	0.3	26	4.5

## Conclusions

The linearity of the responsivity of a SiC detector was investigated at the wavelength of 254 nm, nearby the transition wavelength of the intercombination line of mercury. Coherent ultraviolet radiation was produced by means a SFG process in a BBO crystal, with a power at the desired wavelength variable between 50 and 300 nW. In this exposure range, the detector was determined to be linear within the uncertainty of  $4 \times 10^{-5}$  ( $1\sigma$ ), which is vastly dominated by the statistical contribution. This feature ensures high spectral fidelity in the observation of the Hg absorption spectrum at this wavelength, thus satisfying one of the requirements for the implementation of low-uncertainty Doppler broadening thermometry in the deep-UV. The upper limit to the non-linearity can be further reduced by means of an active stabilization of the ultraviolet power, so that it would be possible to avoid the normalization to the monitor signal, circumstance that would reduce the measurement uncertainty on the linearity factor.

- 1) Kandula D Z, Gohle C, Pinkert T J, Ubachs W and Eikema K S E 2010 Extreme ultraviolet frequency comb metrology *Phys. Rev. Lett.* **105** 063001
- 2) Cingöz A, Yost D C, Allison T K, Ruehl A, Fermann M E, Hartl I and Ye J 2012 Direct frequency comb spectroscopy in the extreme ultraviolet *Nature* **482** 68–71
- 3) Seres J, Seres E, Serrat C, Young E C, Speck J S and Schumm T 2019 All-solid-state VUV frequency comb at 160 nm using high-harmonic generation in non-linear femtosecond enhancement cavity *Opt. Express* **27** 6618–28
- 4) Altmann R K, Dreissen L S, Salumbides E J, Ubachs W and Eikema K S E 2018 Deep-ultraviolet frequency metrology of H<sub>2</sub> for tests of molecular quantum theory *Phys. Rev. Lett.* **120** 043204
- 5) Cheng C-F et al 2018 Dissociation energy of the hydrogen molecule at 10<sup>−9</sup> accuracy *Phys. Rev. Lett.* **121** 013001
- 6) Tyumenev R et al 2016 Comparing a mercury optical lattice clock with microwave and optical frequency standards *New J. Phys.* **18** 113002
- 7) Hachisu H, Miyagishi K, Porsev S G, Derevianko A, Ovsiannikov V D, Pal'chikov V G, Takamoto M and Katori H 2008 Trapping of neutral mercury atoms and prospects for optical lattice clocks *Phys. Rev. Lett.* **100** 053001
- 8) Roseband T et al 2008 Frequency ratio of Al<sup>+</sup> and Hg<sup>+</sup> Single-ion optical clocks; metrology at the 17th decimal place *Science* **319** 1808
- 9) Curtis L J, Irving R E, Henderson M, Matulioniene R, Froese Fischer C and Pinnington E H 2001 Measurements and predictions of the 6s6p <sup>1</sup>,<sup>3</sup>P<sup>1</sup> lifetimes in the Hg isoelectronic sequence *Phys. Rev. A* **63** 042502
- 10) Truong G-W, May E F, Stace T M and Luiten A N 2011 Quantitative atomic spectroscopy for gas thermometry *Phys. Rev. A* **83** 033805
- 11) Truong G-W, Anstie J D, May E F, Stace T M and Luiten A N 2015 Accurate lineshape spectroscopy and the Boltzmann constant *Nat. Commun.* **6** 8345
- 12) Gianfrani L 2016 Linking the thermodynamic temperature to an optical frequency: recent advances in Doppler broadening thermometry *Philos. Trans. R. Soc. A* **374** 20150047
- 13) Matthus C D, Erlbacher T, Burenkov A, Bauer A J and Frey L 2015 Ion implanted 4H-SiC UV pin-diodes for solar radiation detection - simulation and characterization *Mater. Sci. Forum.* **858** 1032–5
- 14) Prasai D, John W, Weixelbaum L, Krüger O, Wagner G, Sperfeld P, Nowy P, Friedrich D, Winter P and Weiss T 2013 Highly reliable silicon carbide photodiodes for visible-blind ultraviolet detector applications *J. Mater. Res.* **28** 33–37
- 15) Thompson A and Chen H M 1994 Beamcom III, a linearity measurement instrument for optical detectors *J. Res. Natl Inst. Stand. Technol.* **99** 751–5
- 16) Corredera P, Hernanz M L, González-Herráez M and Campos J 2003 Anomalous non-linear behaviour of InGaAs photodiodes with overfilled illumination *Metrologia* **40** S150-3
- 17) Yoon H W, Butler J J, Larason T C and Eppeldauer G P 2003 Linearity of InGaAs photodiodes *Metrologia* **40** S154-8
- 18) Sanders C L 1972 Accurate measurements of and corrections for nonlinearities in radiometers *J. Res. Natl Bur. Stand. A* **76** 437–53
- 19) Alins J, Gustafsson U, Somesfalean G and Svanberg S 2000 Sum-frequency generation with a blue diode laser for mercury spectroscopy at 254 nm *Appl. Phys. Lett.* **76** 1234–6
- 20) Boyd G D and Kleinman D A 1969 Parametric interaction of focused Gaussian light beams *J. Phys. D: Appl. Phys.* **39** 3597
- 21) Budde W 1982 large-flux-ratio linearity measurements on Si photodiodes *Appl. Opt.* **21** 3699–701
- 22) Fasci E, De Vizia M D, Merlone A, Moretti L, Castrillo A and Gianfrani L 2015 The Boltzmann constant from the H<sub>2</sub>18O vibration–rotation spectrum: complementary tests and revised uncertainty budget *Metrologia* **52** S233-S241
- 23) Theocharous E 2012 Absolute linearity measurements on a PV HgCdTe detector in the infrared *Metrologia* **49** S99-S104